Constraints on neutron skin thickness and nuclear deformations using relativistic heavy-ion collisions from STAR*

Haojie Xu (For the STAR collaboration)

School of Science, Huzhou University, Huzhou, Zhejiang 313000, China

Received August 2, 2022

In these proceedings, we present the measurements of neutron skin thickness and nuclear deformation using isobar $^{96}_{44}$Ru+$^{96}_{44}$Ru and $^{96}_{40}$Zr+$^{96}_{40}$Zr collisions at $\sqrt{s_{\mathrm{NN}}} = 200$ GeV by the STAR detector. The significant deviations from unity of the isobar ratios of elliptic flow v_2, triangular flow v_3, mean p_{T} fluctuations $\langle \delta p_{\mathrm{T}}^2 \rangle / \langle p_{\mathrm{T}} \rangle^2$, and asymmetric cumulant $\mathrm{ac}_2\{3\}$ indicate large differences in their quadrupole and octuple deformations. The significant deviations of the isobar ratios of produced hadron multiplicity N_{ch}, mean transverse momentum $\langle p_{\mathrm{T}} \rangle$, and net charge number ΔQ indicate a halo-type neutron skin for the Zr nucleus, much thicker than for the Ru nucleus, consistent with nuclear structure calculations. We discuss how we extract the neutron skin thickness, the symmetry energy slope parameter, and deformation parameters from data.

1. Introduction

The isobar collisions, $^{96}_{44}$Ru+$^{96}_{44}$Ru and $^{96}_{40}$Zr+$^{96}_{40}$Zr, were originally proposed to search for the chiral magnetic effect (CME) [1]. Based on the blind analysis with about 2 billion minimum-bias events for each species collected by the STAR experiment, the initial premise of isobar collisions for CME search was not realized [2]. The CME-related backgrounds were found to differ between isobar collisions [2], suggesting sizeable nuclear structure differences between the two isobar nuclei. Those nuclear structure differences and their consequences in experimental observables had been predicted by energy density functional theory (DFT) calculations [3, 4]. Owing to the large statistics collected by the STAR detector and robust cancellation of systematic uncertainties on the observable ratio $R(X) \equiv \frac{X_{\mathrm{RuRu}}}{X_{\mathrm{ZrZr}}}$, isobar collisions provide novel and accurate means to constrain the nuclear structures and strong force parameters.

* Presented at Quark Matter 2022

Nuclear deformation, a ubiquitous phenomenon for most atomic nuclei, reflects collective motion induced by the interaction between valence nucleons and shell structure. In most cases, the deformation has a quadrupole shape that is characterized by overall strength β_2 and triaxiality γ, and/or an octuple shape β_3. In relativistic collisions of two nuclei such deformations enhance the fluctuations of bulk observables that are sensitive to initial state geometry [5]. The deformation parameters can be constrained from the precision measurements of the ratios between two isobar systems of harmonic anisotropy coefficients v_2, v_3, mean transverse momentum $[p_{\mathrm{T}}]$ fluctuations (mean, variance and skewness), and their Pearson correlation coefficient $\rho(v_2^2\{2\}, [p_{\mathrm{T}}])$ [6]. Similar analysis has been performed in Au+Au and U+U collisions [7, 8].

Neutron skin thickness Δr_{np} ($\equiv \sqrt{\langle r_n^2\rangle} - \sqrt{\langle r_p^2\rangle}$, the root mean square difference between neutron and proton distributions) of nuclei can infer nuclear symmetry energy. Such information is of critical importance to the equation of state of dense nuclear matter in neutron stars. Δr_{np} has traditionally been measured in low-energy hadronic and nuclear scattering experiments. Recent measurement using parity-violating electroweak interactions by the PREX-II experiment has yielded a large neutron skin thickness of Pb nucleus [9], at tension with the world-wide data established in hadronic collisions. In isobar collisions at relativistic energies, neutron skin was predicted [3, 4] to affect event multiplicity and elliptic anisotropy. Measurements of those quantities can, in turn, offer an unconventional and perhaps more precise means to probe the neutron skin [10]. Specifically, the ratios between isobar collisions of the produced hadron multiplicities (N_{ch}) [10], the mean transverse momenta ($\langle p_{\mathrm{T}}\rangle$) [11], and the net charge multiplicities (ΔQ) [12] can probe the neutron skin difference between the isobar nuclei.

2. Nuclear deformation measurements in isobar collisions

Anisotropic flow in most central collisions is exquisitely sensitive to nuclear deformation. The deviations of $R(v_2)$ and $R(v_3)$ from unity observed in most central isobar collisions [2] indicate a large quadrupole deformation in Ru nucleus and a large octuple deformation in Zr nucleus [5]. Figure 1 shows the $R(v_2)$ and $R(v_3)$ as a function of charged track multiplicity ($N_{\mathrm{trk}}^{\mathrm{offline}}$) with $|\eta| < 0.5$. We simulate events by a multi-phase transport (AMPT) model with varying β_2 for Ru (and fixed $\beta_2 = 0.06$ for Zr) and varying β_3 for Zr (and fixed $\beta_3 = 0$ for Ru) to match the data to extract the best parameter values. The extracted quadrupole deformation parameter for Ru is $\beta_{2,Ru} = 0.16 \pm 0.02$ and the octuple deformation parameter for Zr is $\beta_{3,Zr} = 0.20 \pm 0.02$. The AMPT results with those deformation parameters are also shown in Fig. 1. Those deformation parameters extracted from isobar collisions are consistent with the measurements from traditional nuclear structure experiments [13, 14]. We also show in Fig. 1 right panel the isobar ratios of mean p_{T} fluctuations $R(\langle \delta p_{\mathrm{T}}^2 \rangle / \langle p_{\mathrm{T}} \rangle^2)$. The trend can be qualitatively described by the Glauber model with the deformation parameters for Ru and Zr.

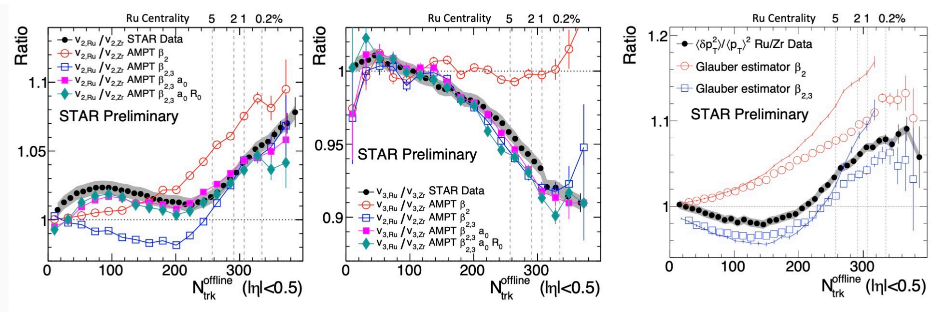

Fig. 1. The $R(v_2)$ (left), $R(v_3)$ (middle), and $R(\langle \delta p_{\mathrm{T}}^2 \rangle / \langle p_{\mathrm{T}} \rangle^2)$ (right) as a function of $N_{\mathrm{trk}}^{\mathrm{offline}}$ in isobar collisions at $\sqrt{s_{\mathrm{NN}}} = 200$ GeV.

The multi-particle correlations are also sensitive to nuclear deformation. In Fig. 2, we present the difference between isobar collisions of the three-particle asymmetric cumulant $\mathrm{ac}_2\{3\}$. Here $\mathrm{ac}_2\{3\} \equiv \langle\langle e^{i(2\varphi_1 + 2\varphi_2 - 4\varphi_3)} \rangle\rangle$ is the average of three-particle azimuthal correlations over an ensemble of events. The $R(\mathrm{ac}_2\{3\})$ trend is similar to that of $R(\langle v_2^4 \rangle)$ as shown in Fig. 2. The double ratio shown in the bottom panel of Fig. 2 indicates that the non-linear response coefficients $\chi_{4,22} = \mathrm{ac}_2\{3\}/\langle v_2^4 \rangle$ are almost identical for the two isobar systems. Both the trends of $R(\mathrm{ac}_2\{3\})$ and $R(\chi_{4,22})$ can be reproduced by the AMPT model simulations. The $R(\mathrm{ac}_2\{3\})$ data, being extra sensitive to flow fluctuations, can help further constrain the deformation parameters of isobar nuclei [15].

3. Neutron skin measurements

Nuclear density distributions, and thus the neutron skin thicknesses, depend on the slope parameter L of symmetry energy as a function of nuclear density. With a given L of the nuclear interaction potential, the nuclear density can be calculated by the DFT framework. The event multiplicity produced in heavy-ion collisions is sensitive to the density distributions of the colliding nuclei, and thus the L. In Fig. 3, we present the ratio of the multiplicity distributions measured in isobar collisions within pseudo-rapidity $|\eta| < 1$, and those computed by the Monte Carlo (MC) Glauber model with the density distributions calculated by DFT with three

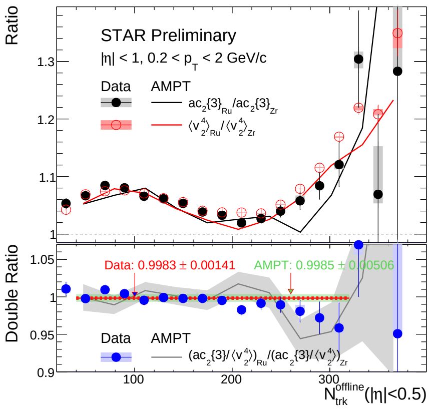

Fig. 2. The three-particle asymmetry cumulant ratio $R(\mathrm{ac}_2\{3\})$ (top) and nonlinear response coefficient ratio $R(\chi_{4,22})$ (bottom) as a function of $N_{\mathrm{trk}}^{\mathrm{offline}}$ in isobar collisions at $\sqrt{s_{\mathrm{NN}}} = 200$ GeV. AMPT simulations are also shown for comparison.

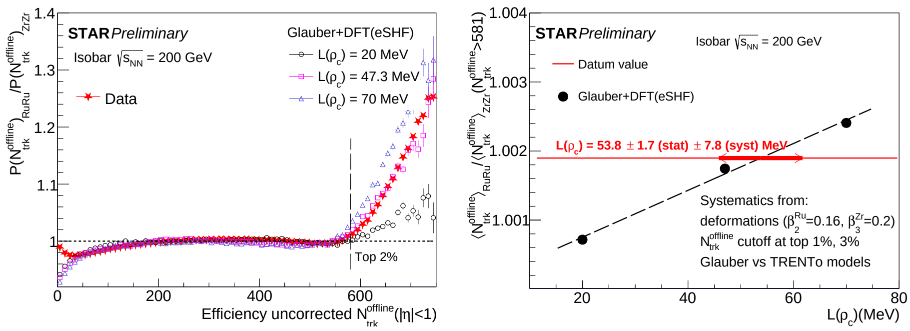

Fig. 3. Left: Ratio of the measured multiplicity ($N_{\mathrm{trk}}^{\mathrm{offline}}$) distributions in isobar collisions at $\sqrt{s_{\mathrm{NN}}} = 200$ GeV. Also shown are Monte Carlo Glauber model results with nuclear densities calculated by DFT with three $L(\rho_c)$ values. Right: Ratio of $\langle N_{\mathrm{trk}}^{\mathrm{offline}} \rangle$ in top 2% central collisions as function of $L(\rho_c)$ from Glauber model. The red line is the measured datum value 1.0019 with statistical uncertainties smaller than 0.0001.

values of $L(\rho_c)$ [10], where $\rho_c = 0.11\rho_0/0.16 \simeq 0.11$ fm^{-3} is nuclear subsaturation cross density. The model result with $L(\rho_c) = 47.3$ MeV can reasonably describe the data including the high multiplicity range. In the right panel of Fig. 3 we compare the ratios of mean multiplicity at top 2% centrality between data and model calculations and obtain $L(\rho_c) = 53.8 \pm 1.7(\mathrm{stat.}) \pm 7.8(\mathrm{sys.})$ MeV. The corresponding neutron skin thicknesses for Ru and Zr are $(\Delta r_{\mathrm{np}})_{\mathrm{Ru}} = 0.051 \pm 0.009$ fm and $(\Delta r_{\mathrm{np}})_{\mathrm{Zr}} = 0.195 \pm 0.019$ fm, respectively. The systematic uncertainties are estimated with different models (TRENTo vs. Glauber) and different $N_{\mathrm{trk}}^{\mathrm{offline}}$ cutoffs, and considering nuclear deformations which are the dominant contribution.

The mean transverse momentum $\langle p_{\mathrm{T}} \rangle$ also depends on the size of the colliding nuclei. The sensitivity is the strongest in most central collisions.

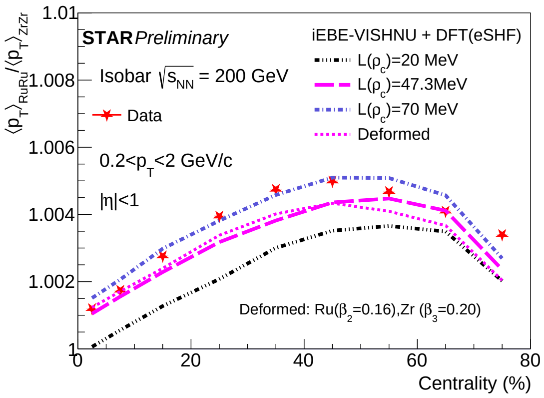

Fig. 4. The mean transverse momentum ratio $R(\langle p_{\rm T}\rangle)$ as a function of centrality in isobar collisions at $\sqrt{s_{\rm NN}}$ = 200 GeV. The three thick curves are obtained from iEBE-VISHNU simulations with three different $L(\rho_c)$ values, the thin-dashed curve denotes the model simulation with $\beta_{2,\rm Ru}$ = 0.16 and $\beta_{3,Zr}$ = 0.20 under $L(\rho_c) = 47.3$ MeV.

This provides another way to constrain the $L(\rho_c)$ parameter. Although $\langle p_{\rm T}\rangle$ depends on bulk properties of the QGP medium, the $R(\langle p_{\rm T}\rangle)$ in isobar collisions shows weak sensitivity to shear and bulk viscosities of the QGP medium [11]. The $R(\langle p_{\rm T}\rangle)$ as a function of centrality is shown in Fig. 4. The trend can be described by iEBE-VISHNU (Event-By-Event Viscous Israel Stewart Hydrodynamics and UrQMD) model simulations, with the nuclear densities obtained from the state-of-art energy density functional theory [10, 16]. Based on the $R(\langle p_{\rm T}\rangle)$ values at top 5% centrality, we extract the slope parameter $L(\rho_c) = 56.8 \pm 0.4(\text{stat.}) \pm 10.4(\text{sys.})$ MeV, and the corresponding neutron skin thicknesses of the isobar nuclei of $(\Delta r_{\rm np})_{\rm Ru} = 0.052 \pm 0.012$ fm and $(\Delta r_{\rm np})_{\rm Zr} = 0.202 \pm 0.024$ fm. The systematic uncertainties are also dominated by the nuclear deformation effect which can be improved in the future. The results extracted from $\langle p_{\rm T}\rangle$ are consistent with those from multiplicity distributions above.

We compare in Fig. 5 our $L(\rho)$ (the slope parameter of symmetry energy at saturation density ρ_0) results with a compilation of world data from traditional nuclear structure experiments [17]. Our results are consistent with world data with comparable precision.

4. Summary

The isobar ${}^{96}_{44}$Ru+${}^{96}_{44}$Ru and ${}^{96}_{40}$Zr+${}^{96}_{40}$Zr collision data collected by STAR at $\sqrt{s_{\rm NN}}$ = 200 GeV provide novel means to probe the nuclear structure and deformation of the isobar nuclei. From the isobar ratios of the measured anisotropic flow, multiplicity, and mean transverse momentum, with the help of DFT calculations, we have extracted the nuclear deformation parameters β_2, β_3, and neutron skin thicknesses $\Delta r_{\rm np}$ of the isobar nuclei, and the density slope parameter of symmetry energy $L(\rho_c)$. The results are consistent with world-wide data from traditional nuclear scattering experi-

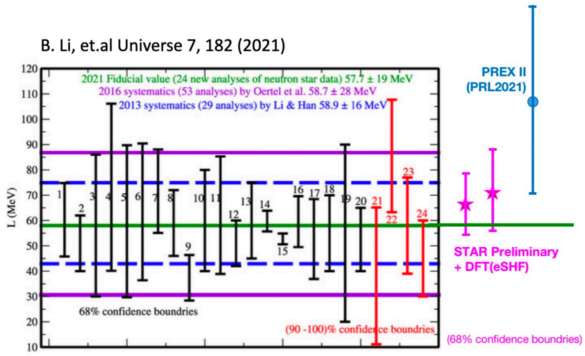

Fig. 5. The compilation of world data of $L(\rho)$ from Ref. [17]. The $L(\rho_c)$ values extracted from isobar data are converted into $L(\rho)$ for comparison. The PREX-II data are taken from Ref. [9]

ments with comparable precision.

This work was supported in part by the National Natural Science Foundation of China under Grant Nos. 11905059, 12035006, 12075085.

REFERENCES

[1] S. A. Voloshin, Phys. Rev. Lett. **105**, 172301 (2010).
[2] M. Abdallah *et al.* (STAR Collaboration), Phys. Rev. C **105**, 014901 (2022).
[3] H. j. Xu, X. Wang, H. Li *et al.*, Phys. Rev. Lett. **121**, 022301 (2018).
[4] H. Li, H. j. Xu, J. Zhao *et al.*, Phys. Rev. C **98**, no.5, 054907 (2018).
[5] C. Zhang and J. Jia, Phys. Rev. Lett. **128**, 022301 (2022).
[6] J. Jia and C. J. Zhang, [arXiv:2111.15559 [nucl-th]].
[7] J. Jia, S. Huang and C. Zhang, Phys. Rev. C **105**, 014906 (2022).
[8] C. Zhang [STAR], [arXiv:2203.13106 [nucl-ex]].
[9] D. Adhikari *et al.* (PREX Collaboration), Phys.Rev.Lett. **126**, 172502 (2021).
[10] H. Li, H. j. Xu, Y. Zhou *et al.*, Phys. Rev. Lett. **125**, 222301 (2020).
[11] H. j. Xu, W. Zhao, H. Li *et al.*, [arXiv:2111.14812 [nucl-th]].
[12] H. j. Xu, H. Li, Y. Zhou *et al.*, Phys. Rev. C **105**, L011901 (2022).
[13] T. Kibédi and R. h. Spear, Atom. Data Nucl. Data Tabl. **80**, 35-82 (2002).
[14] B. Pritychenko, M. Birch, B. Singh and M. Horoi, Atom. Data Nucl. Data Tabl. **107**, 1-139 (2016) [erratum: *ibid.* **114**, 371-374 (2017)].
[15] S. Zhao, H. j. Xu, Y. X. Liu and H. Song, [arXiv:2204.02387 [nucl-th]].
[16] Z. Zhang and L. W. Chen, Phys. Rev. C **94**, no.6, 064326 (2016).
[17] B. A. Li, B. J. Cai, W. J. Xie and N. B. Zhang, Universe **7**, no.6, 182 (2021).